THE JOURNAL OF BIOLOGICAL CHEMISTRY
Vol. 275, No. 46, Issue of November 17, pp. 36436–36440, 2000
Printed in U.S.A.

Alternate Aggregation Pathways of the Alzheimer β-Amyloid Peptide

AN *IN VITRO* MODEL OF PREAMYLOID*

Received for publication, June 28, 2000, and in revised form, August 23, 2000
Published, JBC Papers in Press, August 28, 2000, DOI 10.1074/jbc.M005698200

T. H. Jackson Huang‡§, Dun-Sheng Yang¶, Paul E. Fraser‡¶‖, and Avijit Chakrabartty‡

From the ‡Division of Molecular and Structural Biology, Ontario Cancer Institute and Department of Medical Biophysics, University of Toronto, 610 University Avenue, Toronto, Ontario M5G 2M9, Canada and the ¶Center for Research in Neurodegenerative Disease, University of Toronto, Toronto, Ontario M5S 3H2, Canada

Deposition of amyloid-β (Aβ) aggregates in the brain is a defining characteristic of Alzheimer's disease (AD). Fibrillar amyloid, found in the cores of senile plaques, is surrounded by dystrophic neurites. In contrast, the amorphous Aβ (also called preamyloid) in diffuse plaques is not associated with neurodegeneration. Depending on the conditions, Aβ will also form fibrillar or amorphous aggregates *in vitro*. In this present study, we sought to characterize the properties of the amorphous aggregate and determine whether we could establish an *in vitro* model for amorphous Aβ. CD data indicated that Aβ40 assembled to form either a β-structured aggregate or an unfolded aggregate with the structured aggregate forming at high peptide concentrations and the unstructured aggregate forming at low Aβ40 levels. The critical concentration separating these two pathways was 10 μM. Fluorescence emission and polarization showed the structured aggregate was tightly packed containing peptides that were not accessible to water. Peptides in the unstructured aggregate were loosely packed, mobile, and accessible to water. When examined by electron microscopy, the structured aggregate appeared as protofibrillar structures and formed classic amyloid fibrils over a period of several weeks. The unstructured aggregate was not visible by electron microscopy and did not generate fibrils. These findings suggest that the unstructured aggregate shares many properties with the amorphous Aβ of AD and that conditions can be established to form amorphous Aβ *in vitro*. This would allow for investigations to better understand the relationship between fibrillar and amorphous Aβ and could have significant impact upon efforts to find therapies for AD.

Amyloid deposits, composed primarily of the amyloid-β (Aβ)[1] peptide, are associated with the neuropathology of Alzheimer's disease (AD). Although the precise nature of the relationship between this 39–43-residue peptide and neurodegeneration is still under investigation, a growing body of evidence supports the idea that Aβ plays a primary causal role in the progression of the disease (1–3).

Aβ is a proteolytic product of the β-amyloid precursor protein. β-Amyloid precursor protein is a large type-1 transmembrane protein, is encoded on chromosome 21, and is constitutively expressed in many cell types (4–6). Aβ assembles in a nucleation-dependent process to form intermediate protofibrils and ultimately fibrils 60–90 Å in diameter (7–9). Staining with Congo red and examination under polarized light produces green birefringence (10) indicating that amyloid deposits are composed of peptide polymers with β-sheet structure. This conformational characteristic of Aβ fibrils is confirmed by x-ray diffraction analysis, which shows a cross-β-fiber diffraction pattern with a distance between polypeptide chains of 4.76 Å and a distance between sheets of 10.6 Å (11).

Fibrils are the main component of amyloid deposits known as senile plaques. Senile plaques are lesions 10–200 μm in diameter with a dense core of fibrillar amyloid. These plaques are surrounded by degenerating and swollen nerve terminals (12).

A second type of Aβ deposit found in AD brains is known as diffuse plaques. Unlike senile plaques, diffuse plaques contain little or no fibrillar Aβ and are instead composed of amorphous Aβ (13). Amorphous Aβ is noncongophillic and is only visible by immunocytochemical methods, suggesting that these deposits lack the ordered β-sheet secondary structure responsible for tinctoral and optical properties of fibrillar amyloid. Diffuse plaques are not surrounded by dystrophic neurites and are not associated with neurodegeneration. It has been postulated that diffuse plaques are precursors to senile plaques and hence amorphous Aβ has also been called "preamyloid." Support for this idea comes from studies with Down's syndrome. Patients with this disorder have three copies of chromosome 21 and exhibit extensive Aβ deposition in their brains (14). There appears to be an age-dependent progression from the amorphous Aβ deposits found in the brains of young Down's syndrome subjects to the formation of senile plaques by adulthood (15, 16).

If amorphous Aβ is the progenitor of Aβ fibrils, then it would be of particular usefulness to know what factors drive the conversion from the benign amorphous Aβ of diffuse plaques to the toxic fibrillar amyloid of senile plaques. An important early step in gaining this information would be the establishment of

* The costs of publication of this article were defrayed in part by the payment of page charges. This article must therefore be hereby marked "*advertisement*" in accordance with 18 U.S.C. Section 1734 solely to indicate this fact.

§ Supported by Medical Research Council Grant ME-14865 and funds from Neurochem, Inc.

‖ Supported by funds from Ontario Mental Health Foundation, the Scottish Rite Charitable Foundation, Neurochem, Inc., and the Alzheimer Society of Ontario.

** Supported by a Medical Research Council doctoral award. To whom correspondence should be addressed: Div. of Molecular and Structural Biology, Ontario Cancer Inst. and Dept. of Medical Biophysics, University of Toronto, 610 University Ave., Toronto, ON M5G 2M9, Canada. Tel.: 416-946-2000, Ext. 4910; Fax: 416-946-6529; E-mail: chakrab@oci.utoronto.ca.

[1] The abbreviations used are: Aβ, amyloid-β; AD, Alzheimer's disease; HPLC, high performance liquid chromatography; NBD, 6-(*N*-(7-nitrobenz-2-oxa-1,3-diazol-4-yl)amino)hexanoic acid.

in vitro conditions to form amorphous Aβ aggregates. Aβ fibrillogenesis is a nucleation-dependent process that can be significantly affected by the presence of small peptide aggregates acting as "seeds" (17). In our work we have observed that Aβ preparations in which no special precautions have been taken to eliminate these seeds would form nonspecific aggregates visible by atomic force microscopy (18). We ask the question: could these *in vitro* aggregates be the amorphous Aβ in diffuse plaques?

To answer this question it was important to identify the means by which amorphous Aβ could be recognized. What characteristics distinguish amorphous Aβ from fibrillar amyloid? Although the conformation of Aβ in diffuse plaques is not known, it is likely unstructured. This provides a basis for devising an experimental plan to study amorphous Aβ *in vitro*.

In the present study, we have developed a systematic methodology for identifying diffuse amyloid. Sedimentation was used to determine the aggregation state of Aβ. Subsequently, CD spectroscopy, fluorescence emission, and fluorescence polarization were employed to elucidate the intramolecular and intermolecular structural characteristics of peptides within the aggregates. Finally, the gross morphology of the aggregates was visualized using electron microscopy.

Aggregation is a multi-molecular association reaction and is therefore concentration-dependent. In these experiments, concentration was varied to see how peptide concentration influences Aβ self-association.

If we are able to establish *in vitro* conditions for amorphous Aβ formation, then the methods used here will allow for investigation into the aggregational and secondary structural characteristics of the alternate aggregation pathways of Aβ. These findings will provide a better understanding of the fibril formation process and may have implications in understanding the relationship between diffuse amyloid and amyloid fibrils.

EXPERIMENTAL PROCEDURES

Peptide Synthesis—Peptides were prepared by solid phase synthesis on a PerSeptive Biosystems 9050 Plus peptide synthesizer, as peptide amides using PAL-PEG-PS resin (PerSeptive Biosystems). An active ester coupling procedure, employing *O*-(7-azabenzotriazol-1-yl)-1,1,3,3-tetramethyluronium hexafluorophosphate of 9-fluorenylmethoxycarbonyl amino acids was used. The peptides were cleaved from the resin with 81:13:1:5 trifluoroacetic acid:thioanisole:*m*-cresol: ethanedithiol mixture. After incubation for 1 h at 25 °C, the resin was removed by filtration, and bromotrimethylsilane was added to a final concentration of 12.5% (v/v). After incubation for 5 h at 0 °C, the peptides were precipitated and washed in cold ether and purified by HPLC. Peptide purity and identity was confirmed by electrospray mass spectrometry.

Fluorescent Labeling—Prior to fluorescent labeling, a glycine residue was added to the N terminus of Aβ40 to act as a flexible linker between the fluorophore and peptide. 6-(*N*-(7-Nitrobenz-2-oxa-1,3-diazol-4-yl)amino)hexanoic acid (NBD) (Molecular Probes) was then coupled to this extended Aβ40 sequence during peptide synthesis to create NBD-Aβ40. Peptide purity and identity was confirmed by electrospray mass spectrometry.

Preparation of Stock Peptide Solutions and Concentration Determination—Aβ40 and NBD-Aβ40 preparations were lyophilized then dissolved in 10% hexafluoro-2-propanol. Peptide concentration was determined by tyrosine absorbance at 275 nm (ϵ = 1390 cm^{-1} M^{-1}) (20) for Aβ40 and by NBD absorbance at 480 nm (ϵ = 23,000 cm^{-1} M^{-1}) (21). Absorbance measurements were made on a PerkinElmer Life Sciences Lambda 3B spectrophotometer. The stock solutions were stored at −20 °C until required. During the course of the experiments, stock peptide solutions were stored for several weeks; no changes in the behavior of these peptides were observed over this time.

Electron Microscopy—Negatively stained fibrils were prepared by floating charged pioloform, carbon-coated grids on peptide solutions. These solutions were incubated for 8 weeks. To control pH, the peptide solutions were made using a 25 mM phosphate buffer. After the grids were blotted and air-dried, the samples were stained with 1% (w/v) phosphotungstic acid.

Platinum/carbon shadowing was performed using the glycerol spray method (19). Solutions containing Aβ40 were brought to 30–50% (v/v) glycerol, sprayed onto freshly cleaved mica, and freeze-dried. The preparations were shadowed on an Edwards E12E4 coater with platinum/carbon (15–20 Å) at an angle of 5–7° followed by an additional 30–40 Å of carbon-coating applied at an angle of 90°. Film deposition was measured with a Balzers QSE201 quartz crystal monitor. The platinum/carbon replicants were floated off in distilled water and placed onto 300-mesh copper grids. Representative electron microscopy images of the peptide assemblies were acquired on a Hitachi H-7000 TEM operated with an accelerating voltage of 75 kV.

Fluorescence Emission Spectroscopy—Steady-state fluorescence was measured at room temperature using a Photon Technology International QM-1 fluorescence spectrophotometer equipped with excitation intensity correction and a magnetic stirrer. For measurements of NBD fluorescence, emission spectra from 500 to 600 nm were collected (λ_{ex} = 470 nm, averaging time = 0.1 or 1 s, 1-nm steps, bandpass = 4 nm for excitation and emission). A quartz cuvette with 1-cm path length and 0.5-ml volume was used. Spectra of samples containing only unlabeled Aβ40 were used to correct for light scattering.

Samples were prepared with a fixed concentration of 0.1 μM NBD-Aβ40 as a tracer. Stock peptides were mixed then diluted to the desired final concentrations and pH using buffer (25 mM borate, 25 mM citrate, and 25 mM phosphate). After dilution, the pH was again measured and readjusted, if necessary, and then all samples were incubated 18–24 h prior to spectral acquisition.

Fluorescence Depolarization Spectroscopy—For steady-state polarization experiments, the fluorescence spectrophotometer was configured in the L format, and samples of NBD-Aβ40 and free NBD were excited at 478 nm. The intensities (I) of the vertical (v) and horizontal (h) components of emission at 530 nm were measured. Fluorescence polarization (p) was calculated according to the equation, $p = (I_{vv} - GI_{vh})/(I_{vv} + GI_{vh})$ where first and second subscripts refer to the positions of the excitation and emission polarizers, respectively, and $G = I_{hv}/I_{hh}$. G is the factor used to correct for detection differences between vertically and horizontally polarized light. A concentration series of Aβ40 was prepared (0.75, 1.5, 3, 6, 12, 24, and 48 mM Aβ40 with 0.1 μM NBD-Aβ40, 25 mM phosphate, pH 7.0), and the fluorescence polarization of the samples was measured.

Circular Dichroism Spectroscopy—CD spectra were recorded on an Aviv Circular Dichroism Spectrometer model 62DS at 25 °C. Spectra were obtained from 200 to 300 nm (0.5-cm path length, 0.5-nm steps, and 1-nm bandwidth) on a sample containing 20 μM Aβ40 in buffer (7.5 mM borate, 7.5 mM citrate, and 7.5 mM phosphate).

RESULTS

For the experiments we chose to use the 40-residue form of Aβ (Aβ40). This synthetic peptide was HPLC purified, but no attempt was made to remove aggregates or fibril seeds that may have been present. Aβ40 contains no intrinsic fluorophores; thus, it was necessary to introduce an extrinsic fluorescent molecule. This was accomplished by attaching the environment-sensitive fluorophore, NBD, to the N terminus of Aβ40 via two glycine residues. These glycines act as a flexible linker to prevent any adverse steric effects that may have been exerted by NBD. This labeled molecule, NBD-Aβ40, was then added as a tracer to samples made with Aβ40. This approach has the distinct advantage that most of the peptide would be wild type, whereas only a tiny component would be the engineered molecule.

Concentration Effect on Aβ40 Aggregation—Samples with fixed tracer amounts of labeled peptide (0.1 μM NBD-Aβ40) and increasing concentrations of unlabeled peptide (were prepared at pH 7 and allowed to incubate overnight. Sedimentation by centrifugation was used to test for the formation of Aβ40 aggregates.

The absorbance of NBD at 490 nm was measured before centrifugation (Fig. 1). The samples were then centrifuged, and the NBD absorbance was measured again. After centrifugation little if any NBD absorbance remained at all concentrations. Thus, sedimentable aggregates formed at all peptide concentrations. It was possible to pellet the aggregate in a table top centrifuge set at 15,600 × g, a relatively slow speed. This suggested that the aggregates were large. Furthermore, be-

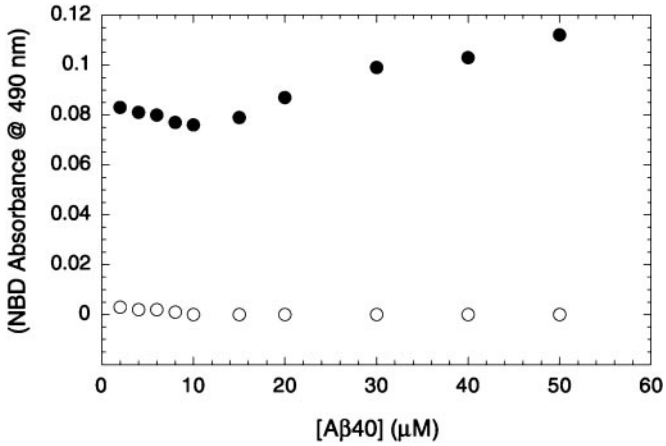

FIG. 1. **The NBD absorbances of Aβ40 samples (0–50 μM Aβ40, 0.1 μM NBD-Aβ40, 25 mM phosphate, pH 7.0) were measured before (●) and after (○) centrifugation for 30 min at 15,600 × *g*.** Prior to centrifugation, absorbance at 490 nm remained relatively constant around 0.08 for concentrations up to 15 μM. By 20 μM Aβ40, absorbance increased with increasing concentration. After centrifugation, nearly all of the absorbance at every concentration was lost, indicating that most of the Aβ40 was sedimentable.

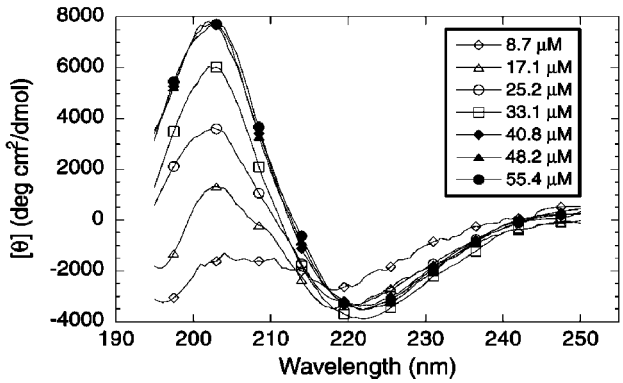

FIG. 2. **Samples of Aβ40 were prepared and incubated overnight (8.7, 17.1, 25.2, 33.1, 40.8, 48.2, and 55.4 μM Aβ40, 5 mM phosphate, pH 7.0).** The CD spectra also showed a concentration-dependent change. The shape of the spectrum at 8.7 μM suggested that the Aβ40 in the sample contained little, if any, secondary structure. In contrast, the spectrum of the 55.4 μM Aβ40 sample had a negative band at 218 nm and a positive band at around 200 nm, features that indicate β-structure. The extent of β-sheet adopted by Aβ40 evolved as total peptide concentration increased.

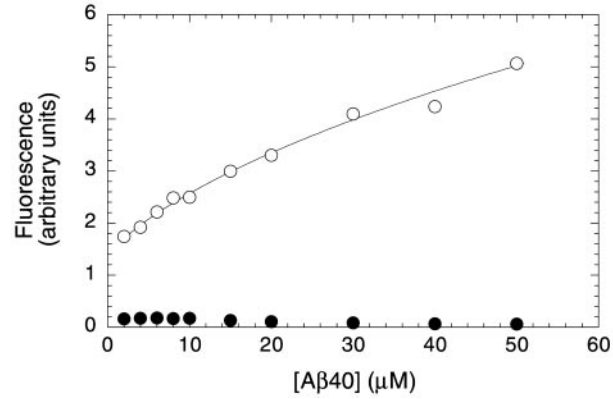

FIG. 3. **The NBD fluorescence of Aβ40 samples (0–50 μM Aβ40, 0.1 μM NBD-Aβ40, 25 mM phosphate, pH 7.0) was measured before (○) and after (●) centrifugation for 30 min at 15,600 × *g*.** The fluorescence measurements showed a concentration dependence with the intensity of NBD fluorescence emission increasing with higher total peptide concentrations. After centrifugation, little fluorescence remained in the sample supernatant, confirming the conclusion from the absorbance experiments that most of the Aβ40 is in the form of large sedimentable aggregates.

cause nearly all absorbance was lost, most of the Aβ40 had aggregated into an insoluble form, and only a small fraction of the peptide remained in solution.

Secondary Structure of Aβ40 Aggregates—The tinctoral properties of amyloid suggest that fibrillar amyloid has ordered structure, whereas amorphous Aβ does not. To see whether there were any differences in secondary structure among the amyloid preparations, CD spectroscopy was used (Fig. 2). The spectrum at lowest peptide concentration (8.7 μM) was representative of an unfolded conformation. Because the sedimentation data showed that most of the Aβ40 is aggregated at this concentration, this suggested that it is the aggregates which were unstructured. At 17.1 μM the spectrum showed characteristics that were representative of β-structure: a positive band around 200 nm and a negative band at 218 nm. By 25.2 μM these bands were quite pronounced. The amount of β-structure content of Aβ40 aggregates reached a maximum by 40.8 μM. Thus, β-structure evolved as the total peptide concentration increased. Light scattering because of the presence of aggregated material can often confound the interpretation of CD spectra. Because most of the peptide in these samples was aggregated, this could have been a significant problem. However, the spectra here closely resembled CD spectra of unfolded and β-sheet conformations. In this case, we are confident light scattering effects have not adversely influenced the results. Thus, Aβ40 formed aggregates at all concentrations tested and there were two distinct types; at low concentration, Aβ40 associated to form unstructured aggregates, whereas at high concentrations, Aβ40 associated to form β-structure aggregates.

In diffuse plaques, amyloid appears wispy and noncompacted, whereas senile plaques appear dense and fibrillar. These morphological characteristics suggest that constituent peptides may have different solvent accessibility depending on whether they are present in diffuse amyloid or fibrillar amyloid. To see whether similar situation existed with our *in vitro* amyloid, we looked at solvent accessibility using NBD as our representative side chain. NBD, having a similar size and shape to Trp, could be accepted into the aggregate/fibril like other aromatic amino acids. Once introduced into Aβ40, any effects of solvent accessibility will act on NBD as with other residues in the sequence with the advantage that any changes would be reported by the fluorescence characteristics of the fluorophore.

Side Chain Environment of Aβ40 Aggregates—The fluorescence of NBD is quenched by water. When NBD-Aβ40 is not assembled, NBD is accessible to water. NBD fluorescence would be quenched, and fluorescence emission in the sample would be low. When Aβ40 assembles, water would be excluded and quenching would be reduced so fluorescence increases. If there were a further conformational change that results in a more compact structure and further sequesters NBD from water, then fluorescence would be further enhanced.

Again a fixed tracer amount of NBD-Aβ40 was used in conjunction with an increasing amount of unlabeled Aβ40. With more Aβ40 there was increased fluorescence emission, suggesting that solvent accessibility decreased with increasing concentration (Fig. 3). This change indicated that the aggregate at low concentration was different from the aggregate that formed at high concentration or, specifically, that Aβ40 aggregates condensed with increasing concentration to form more compact structures that effectively sequestered NBD from quenching by water. If there were no change in structure, then the fluorescence would have remained flat throughout the concentrations.

Centrifugation of the samples and measurement of fluorescence produced results identical to those from the absorbance

measurements. Nearly all the fluorescence in each sample was lost after centrifugation. This confirmed that large sedimentable aggregates formed at all concentrations. Furthermore, that most fluorescence was lost indicated the majority of peptide aggregated, and only a small fraction of Aβ40 comprised the soluble component.

The evidence accumulated thus far supported the idea that we were producing *in vitro* versions of diffuse and fibrillar amyloid as these aggregates shared properties with *in vivo* AD amyloid. The increase in fluorescence was consistent with formation of noncompact structures at low peptide concentration and evolution of tightly packed water excluding structures as protofibrils or fibrils formed with increasing peptide amounts. The mobility of side chains would be further information as to how tightly packed the peptides are in one aggregate type *versus* another. Another property of fluorescence, fluorescence polarization, can be used to investigate this.

Side Chain Mobility of Aβ40 Aggregates—If a fluorophore is excited by polarized light, then the emitted light will also be polarized. The fluorophore will move during the time delay between excitation and emission, and this movement will result in the depolarization of the emitted light relative to the excitation light. The degree of depolarization is dependent on the rotational relaxation time; the greater the rate of rotation, the lower its polarization. In our system, two motions will affect the polarization of the fluorescence emission: global motions and local motions. Any changes in global motions would give information on the aggregation state of NBD-Aβ40, whereas changes in local motions would provide information on the packing state of our representative side chain NBD

The polarization of free NBD was first measured (Fig. 4). This value was relatively low, 0.32, because it is a small molecule and has a short rotational relaxation time. However, once attached to Aβ40, a much larger molecule, its movement was more restricted, and the measured polarization was higher. Polarization increased up to 10 μM then stabilized. The 10 μM Aβ40 concentration may mark a transition between two states. We knew that large aggregates formed at all concentrations; it was unlikely then that the change in polarization was due to global motion changes. Rather, it was more likely that the local motions of NBD were the cause. Thus, above 10 μM, NBD was contained within the β-structure aggregate and was tightly packed and not free to move. 10 μM seems to be critical concentration dividing the conversion between two aggregate types.

Aβ formed two distinct aggregate types: an unstructured aggregate and the β-structured aggregate. Not only is the unstructured aggregate lacking regular secondary structure, but also its conformation is looser, solvent exposed, and its constituent peptides are not as tightly associated. On the other hand, the peptides in the β-structured aggregate showed β-sheet secondary structure, were tightly packed, and excluded water from their side chain environments. These *in vitro* aggregates appeared to share many properties with *in vivo* amyloid forms. As a final step, we attempted to visualize the morphology of the aggregates by employing electron microscopy.

Ultrastructure of Aβ40 Aggregates—Aβ40 preparations were examined by either platinum/carbon shadowing electron microscopy or negative stain electron microscopy. At 0.1 μM NBD-Aβ40 and 5 μM Aβ40 (Fig. 5*A*), a concentration that exhibited aggregate formation but no ordered secondary structure, only a few small spherical structures were present. Although we know that the unstructured aggregate was forming at this concentration, they were not visible by this technique. As the peptide concentration was raised (0.1 μM NBD-Aβ40 and 50 μM Aβ40; Fig. 5*B*), these structures became abundant; moreover, the spherical aggregates seemed to assemble into clusters and elongated aggregates similar to protofibrils. Because CD showed that β-structure evolved with concentration, we concluded that these protofibrils were the β-structure aggregate. After 8 weeks of incubation, the high concentration Aβ40 sample (0.1 μM NBD-Aβ40 and 48 μM Aβ40, Fig. 5*C*) had taken on the morphology of classic amyloid fibrils.

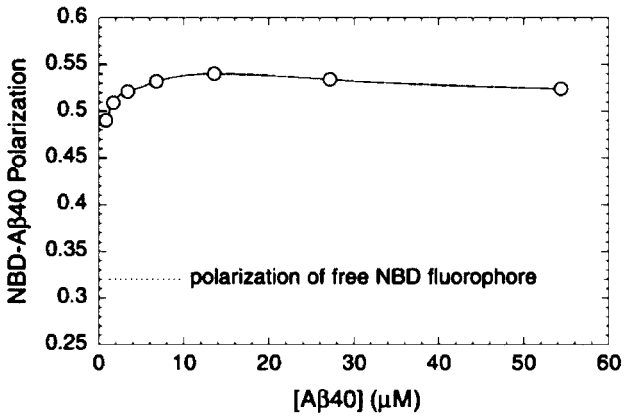

FIG. 4. **A concentration series of Aβ40 was prepared (0.75, 1.5, 3, 6, 12, 24, and 48 μM Aβ40 with 0.1, 0.2, 0.4, 0.8, 1.6, 3.2, and 6.4 μM NBD-Aβ40, 25 mM phosphate, pH 7.0), and the fluorescence polarization of the samples were measured.** Fluorescence polarization was 0.49 at the lowest peptide concentration tested. Polarization increased to a maximum value of 0.54 at 13.6 μM and leveled off up to the highest concentration of 54.4 μM. The polarization of the free NBD fluorophore is shown as a reference (*dotted line*).

DISCUSSION

In the search to identify the neurotoxic species of Aβ in AD, amorphous Aβ has been ignored as a subject of investigation because diffuse plaques are not associated with neurodegen-

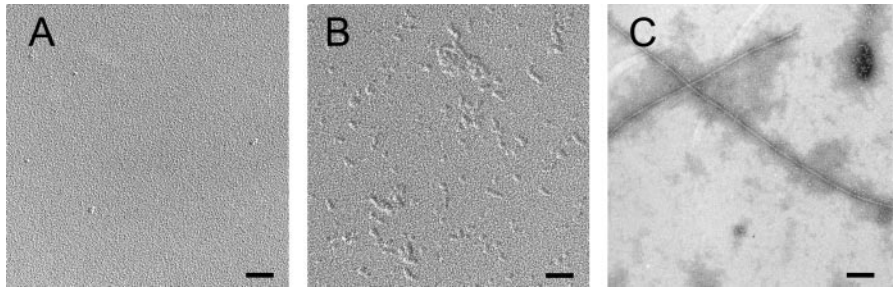

FIG. 5. **Platinum/carbon shadow electron microscopy was performed on samples of Aβ40 at varying concentrations after overnight incubation.** Negative stain electron microscopy was performed on a 48 μM sample that had been incubating for 8 weeks. All samples contained 25 mM phosphate and had a pH of 7.0. *Bars* indicate 100 nm. Some spherical structures were visualized at 0.1 μM NBD-Aβ40 (*A*). As the amount of peptide was increased (*B*; 0.1 μM NBD-Aβ40, 50 μM Aβ40), the number of structures increased. The structures at the higher concentration appeared to be aggregates of the spherical structures that predominated at the lower concentrations and resembled protofibrils. The micrograph of the 8-week-old 0.1 μM NBD-Aβ40, 48 μM Aβ40 sample (*C*) showed that our synthetic peptides formed classic amyloid fibrils under the *in vitro* conditions employed in the experiments.

eration. However, it is clear that amorphous Aβ is an important component of the total amyloid load in the AD brain, and therefore, its properties should be better understood. Previous studies have emphasized the importance of ensuring that preparations of Aβ are seed-free in generating Aβ fibrils rather than nonspecific aggregates (17). We reported previously that peptide stocks that have been carefully pretreated to remove seeds generated soluble oligomeric structures that formed prior to fibrillar amyloid (19). We also observed that Aβ40 preparations where seeds have not been removed formed amorphous aggregates (18). In the present study, we have found that these samples may provide a useful *in vitro* system for studying *in vivo* amorphous Aβ.

Many of the experiments make use of Aβ40 labeled with the fluorescent probe NBD. The behavior of NBD-Aβ40 appears to be comparable with that of Aβ40 itself. We have reported previously that NBD-Aβ40 has similar solubility characteristics (18). Furthermore, under defined conditions, Aβ40 labeled with NBD as well as other fluorescent probes, Trp or 5-acetylethyldiaminonaphthalene-1-sulfonic acid,, self-associates to form oligomeric structures like unlabeled Aβ40 (19). As a final precaution, to reduce the possibility of the fluorophore affecting the behavior of Aβ40, labeled peptide has been used in tracer amounts.

There are at least two different aggregation pathways for Aβ40: one leading to a β-structure aggregate and the other to an unstructured aggregate. The β-structured aggregate is composed of tightly packed Aβ40 peptides that have β-sheet secondary structure and may be the protofibril precursor to Aβ fibrils. The unstructured aggregate lacks regular secondary structure, its constituent peptides are not tightly associated, and its conformation is looser with the side chain solvent exposed. The unstructured aggregate shares many properties with the diffuse amyloid in AD. Whether Aβ40 associates to form the unstructured aggregate or fibrils is determined by the total peptide concentration. The critical concentration separating these two pathways is 10 μM. A possible explanation for why the more compact and ordered fibrils form at higher concentration is that the nucleus for fibril formation is stable only at peptide concentrations above 10 μM.

It has been suggested that there is a time-dependent relationship between amorphous Aβ and fibrillar amyloid where diffuse amyloid is the precursor to fibril formation. Our results show this relationship may not only be one of time but rather one that is also based on concentration. Some mutations associated with AD increase Aβ concentration. This would have the effect of shifting the aggregation pathway to favor formation of β-structured aggregate and hence Aβ fibrils. If fibrils are toxic it would be critical to prevent this step from taking place. A treatment strategy is to reduce Aβ concentration below the critical concentration for conversion to fibrils and thereby maintain amyloid in the non-neurotoxic amorphous form making it unnecessary to completely eliminate Aβ.

It would be useful to examine whether amorphous and fibrillar Aβ directly interconvert, that is, once amorphous Aβ is formed does it convert to fibrillar amyloid? Solid to solid transitions are rare and require extreme conditions such as high pressure in the case of coal-graphite-diamond conversion. It is unlikely that a such a transition is taking place *in vivo*. A more plausible mechanism is that Aβ monomers are the intermediate between these two aggregates. An understanding of this interconversion would be necessary to evaluate whether reducing peptide concentration to control the aggregation pathway would be sufficient to prevent AD pathogenesis.

Alternatively, the aggregation of Aβ into amorphous may generate, by chance, nucleation sites from which structured fibrils can grow with the addition of monomeric Aβ. The present study indicates that concentration is an important factor influencing amyloid morphology; however, the precise mechanisms driving conversion will have to be determined in future experiments.

The methodology used in this study can be deployed to test drugs. Fluorescence techniques can be utilized as a preliminary screen for potential drugs that prevent formation of β-structured aggregates. Subsequently, CD spectroscopy can be applied for confirmation.

Acknowledgment—We thank Sandy Go for technical assistance in synthesizing Aβ40.

REFERENCES

1. Pike, C. J., Burdick, D., Walencewicz, A. J., Glabe, C. G., and Cotman, C. W. (1993) *J. Neurosci.* **13,** 1676–1687
2. Simmons, L. K., May, P. C., Tomaselli, K. J., Rydel, R. E., Fuson, K. S., Brigham, E. F., Wright, S., Lieberburg, I., Becker, G. W., Brems, D. N., and Li, W. Y. (1993) *Mol. Pharmacol.* **45,** 373–379
3. Lorenzo, A., and Yankner, B. (1994) *Proc. Natl. Acad. Sci. U. S. A.* **91,** 12243–12247
4. Kang, J., Lemaire, H.-G., Unterbeck, A., Salbaum, J. M., Masters, C. L., Grzeschik, K. H., Multhaup, G., Beyreuther, K., and Müller-Hill, B. (1987) *Nature* **325,** 733–736
5. Selkoe, D. J., Podlisny, M. B., Joachim, C. L., Vickers, E. A., Lee, G., Fritz, L. C., and Oltersdorf, T. (1988) *Proc. Natl. Acad. Sci. U. S. A.* **85,** 7341–7345
6. Dyrks, T., Weidemann, A., Multhaup, G., Salbaum, J. M., Lemaire, H. G., Kang, J., Muller-Hill, B., Masters, C. L., and Beyreuther, K. (1988) *EMBO J.* **7,** 949–957
7. Jarrett, J. T., and Lansbury, P. J. (1992) *Biochemistry* **31,** 12345–12352
8. Jarrett, J. T., Berger, E. P., and Lansbury, P. T. Jr. (1993) *Biochemistry* **32,** 4693–4697
9. Walsh, D. M., Lomakin, A., Benedek, G. B., Condron, M. M., and Teplow, D. B. (1997) **272,** 22364–22372
10. Puchtler, H., Sweat, F., and Levine, M. (1962) *J. Histochem. Cytochem.* **10,** 355–364
11. Kirschner, D., Abraham, C., and Selkoe, D. (1986) *Proc. Natl. Acad. Sci. U. S. A.* **83,** 503–507
12. Müller-Hill, B., and Beyreuther, K. (1989) *Annu. Rev. Biochem.* **58,** 287–307
13. Yamaguchi, H., Nakazato, Y., Hirai, S., Shoji, M., and Harigaya, Y. (1989) *Am. J. Pathol.* **135,** 593–597
14. Wisniewski, K. E., Dalton, A. J., McLachlan, C., Wen, G. Y., and Wisniewski, H. M. (1985) *Neurology* **35,** 957–961
15. Giaccone, G., Tagliavini, F., Linoli, G., Bouras, C., Frigerio, L., Frangione, B., and Bugiani, O. (1989) *Neurosci. Lett.* **97,** 232–238
16. Mann, D. M. (1989) *Neurobiol. Aging* **10,** 397–399
17. Walsh, D. M., Hartley, D. M., Kusumoto, Y., Fezoui, Y., Condron, M. M., Lomakin, A., Benedek, G. B., Selkoe, D. J., and Teplow, D. B. (1999) *J. Biol. Chem.* **274,** 25945–25952
18. Yang, D.-S., Yip, C. M., Huang, T. H. J., Chakrabartty, A., and Fraser, P. E. (1999) *J. Biol. Chem.* **274,** 32970–32974
19. Huang, T. H. J., Yang, D.-S, Plaskos, N. P., Go, S., Yip, C. M., Fraser, P. E., and Chakrabartty, A. (2000) *J. Mol. Biol.* **297,** 73–87
20. Edelhoch, H. (1967) *Biochemistry* **6,** 1948–1954
21. Chantler, P. D., and Szent-Gyorgyi, A. G. (1978) *Biochemistry* **17,** 5440–5447